RSC Advances

PAPER

View Article Online
View Journal | View Issue

Cite this: *RSC Adv.*, 2024, **14**, 29014

Optimization of diformylfuran production from 5-hydroxymethylfurfural *via* catalytic oxidation in a packed-bed continuous flow reactor†

Supakrit Pumrod,[a] Nattee Akkarawatkhoosith,[b] Amaraporn Kaewchada,[c] Tiprawee Tongtummachat,[b] Kun-Yi Andrew Lin[de] and Attasak Jaree *[af]

Received 10th August 2024
Accepted 4th September 2024

DOI: 10.1039/d4ra05816j

rsc.li/rsc-advances

DFF's diverse applications in pharmaceuticals, fungicides, and polymer synthesis motivate the development of efficient production methods. This study reports the continuous-flow synthesis of DFF from 5-HMF in a packed-bed reactor. The Box–Behnken design coupled with response surface methodology (RSM) was employed to optimize the reaction parameters (catalyst, solvent, temperature, oxygen flow rate, catalyst amount) for DFF yield. Ru/Al_2O_3 in toluene proved to be the most effective catalyst–solvent combination. The optimal conditions for DFF production were identified as: 140 °C reaction temperature, 10 ml min^{-1} oxygen flow rate, and 0.15 g catalyst loading. Under these conditions, a DFF yield of 84.2% was achieved.

Introduction

The global reliance on fossil fuels and fossil-based chemicals and petrochemical products has resulted in significant carbon dioxide emissions, contributing to global warming. Concerns about climate change and the finite nature of fossil reserves have spurred researchers to seek alternative resources.[1–3] One promising alternative is biomass, which involves converting biological materials into chemicals and fuels. Biomass-derived chemicals, such as 5-hydroxymethylfurfural (5-HMF),[4–6] diformylfuran (DFF),[7] and 2,5-furandicarboxylic acid (FDCA),[8] offer a sustainable alternative to petroleum-based compounds. As versatile building blocks, they can serve as starting reagents in various industries, producing a wide range of consumer goods such as pharmaceuticals, polymers, resins, solvents, fungicides, and biofuels. Among these, 5-HMF stands out for its versatility and potential as a foundational building block for future biorefineries.

Recently, there has been growing interest in producing DFF from 5-HMF due to DFF's diverse industrial applications. DFF is utilized in sectors such as pharmaceuticals, fungicides, organic catalysts, macrocyclic ligands, and as a monomer for multifunctional polymers.[9–12] It can be synthesized from 5-HMF through oxidation or dehydrogenation reactions of the hydroxymethyl group, which require specific reaction conditions to avoid side reactions like excessive oxidation, decarboxylation, ring-opening, and polymerization. For instance, excessive oxidation can lead to by-products such as 5-hydroxymethylfurfural acid (HMFCA) and FDCA.[13–19]

Previous research has used various oxidants, including H_2O_2, NaOCl, and $BaMnO_4$, to synthesize DFF from 5-HMF.[20–22] These methods required precise quantities of oxidants and generated significant waste. Amarasekara *et al.* achieved an 86% DFF yield using Mn(III) salen complexes as catalysts in a buffer–CH_2Cl_2 system at room temperature with NaOCl as the oxidant.[23] However, recovering and reusing both the catalyst and solvent proved challenging, as did separating DFF from the reaction mixture. To address these issues, recent research has increasingly used O_2 or air as oxidants, improving 5-HMF conversion and DFF selectivity. Nonetheless, the use of homogeneous catalysts remains a barrier to industrial scalability. For instance, Partenheimer *et al.* employed homogeneous metal bromide catalysts with acetic acid, achieving a 99.7% 5-HMF conversion and 61% DFF selectivity.[24] Moreau *et al.* used V_2O_5/TiO_2 catalysts at 363 K and 1.6 MPa air pressure with toluene as the solvent, yielding an 85% yield.[25] Corma *et al.* reported an 82% DFF yield using immobilized vanadyl pyridine complexes at 403 K.[1] Despite these successes, product separation from the solvent remains a cost-intensive process, prompting the development of heterogeneous catalysts for DFF synthesis.

[a]*Center of Excellence on Petrochemical and Materials Technology, Department of Chemical Engineering, Faculty of Engineering, Kasetsart University, Chatuchak, Bangkok, Thailand. E-mail: fengasj@ku.ac.th*

[b]*Department of Chemical Engineering, Faculty of Engineering, Mahidol University, Nakhon Pathom, Thailand*

[c]*Department of Agro-industrial, Food, and Environmental Technology, King Mongkut's University of Technology North Bangkok, Bandsue, Bangkok, Thailand*

[d]*Environmental Engineering & Innovation and Development Center of Sustainable Agriculture, National Chung Hsing University, Taichung, Taiwan*

[e]*Institute of Analytical and Environmental Sciences, National Tsing Hua University, Hsinchu, Taiwan*

[f]*Center for High-Value Products from Bioresources (HVPB), Department of Chemical Engineering, Faculty of Engineering, Kasetsart University, Bangkok 10900, Thailand*

† Electronic supplementary information (ESI) available. See DOI: https://doi.org/10.1039/d4ra05816j

Noble metals like Pt, Au, and Ru have been used as catalysts for oxidizing alcohol functional groups in 5-HMF. For example, Takagaki *et al.* used Ru(OH)x/HT as a catalyst in *N*,*N*-dimethylformamide (DMF), achieving a 92% DFF yield.[18] Nie *et al.* utilized Ru/C in toluene at 383 K and 2.0 MPa O_2, resulting in a 96% DFF yield.[26] Antonyraj *et al.* reported a 99% conversion and 97% DFF selectivity using Ru/Al_2O_3 at 130 °C and 40 psi O_2 pressure with toluene.[27] However, these studies used batch reactors, which are time-consuming and unsuitable for large-scale applications. Consequently, continuous flow reactors have been adopted to enhance DFF production efficiency. Continuous flow reactors offer reduced operational costs, lower environmental impact, and scalability for industrial use. They also provide flexibility in adjusting reaction times and product properties by varying flow rates or reactant concentrations. Chen *et al.* explored DFF synthesis from 5-HMF using Cu/Al_2O_3 in a continuous flow reactor at 260 °C, achieving a 47.7% conversion and 79.2% DFF selectivity.[28]

In this study, we investigated the synthesis of DFF from 5-HMF using ruthenium supported on Al_2O_3 and platinum supported on activated carbon as catalysts. The use of heterogeneous catalysts facilitates easy separation from the reaction mixture, reusability, and commercial viability, making them suitable for industrial-scale production. Oxygen served as the oxidizing agent, and the reactions were conducted in a continuous flow reactor, ensuring efficient heat and mass transfer with straightforward scalability. Initially, we examined the effects of different catalysts and solvents. Subsequently, we optimized the reaction conditions, including catalyst quantity, reaction temperature, O_2 flow rate, and DFF yield using response surface methodology (RSM).

Methodology

Materials

All chemical reagents used in this work were procured from Sigma-Aldrich, including 5-hydroxymethylfurfural (5-HMF, purity >99%), 5-hydroxymethyl-2-furancarboxylic acid (HMFCA, purity ≥95%), 2,5-diformylfuran (DFF, purity ≥96.5%), 5-formyl-2-furancarboxylic acid (FFCA, purity ≥97%), and 2,5-furandicarboxylic acid (FDCA, purity 97%). Toluene of analytical reagent (AR) grade was obtained from Fisher Scientific. High-performance liquid chromatography (HPLC) grade acetonitrile (ACN) and methanol (MeOH) were utilized for HPLC analysis. Oxygen gas (purity 99.99%), employed as the oxidizing agent, was sourced from Linde (Thailand) PLC. The catalysts employed were 5 wt% metal supported on activated carbon (Ru, Pt/C) and alumina (Ru/Al_2O_3), acquired from Riogen, Inc.

Catalyst characterization

In this investigation, three varieties of catalyst were employed: 5% weight platinum supported on activated carbon, 5% weight ruthenium supported on activated carbon, and 5% weight ruthenium supported on alumina. The catalysts' crystalline structure was assessed *via* X-ray diffraction analysis. The surface properties of the catalysts were evaluated utilizing the N_2 adsorption–desorption technique employing a 3-Flex surface characterization analyzer (Micromeritics Instrument Corporation model ver. 4.04). The specific surface area was determined applying the Brunauer–Emmett–Teller (BET) theory. Additionally, the total pore volume and average pore size were computed using the Barrett–Joyner–Halenda (BJH) method.

Catalytic oxidation of 5-HMF

Fig. 1 illustrates the schematic representation of the experimental setup employed for the synthesis of DFF. A high-pressure syringe pump (ISCO series 260D) and a mass flow controller were utilized for the delivery of 5-HMF solution and oxygen gas, respectively. Prior to entering the reactor, these two streams were combined at the T-mixer. The reactor, comprising a stainless-steel tube with an inner diameter of 0.386 cm, housed the catalyst particles, packed within a length range of 0.5–1.5 cm (0.5–1.5 g). Quartz wool layers were employed at the front and back ends to secure the catalyst in position. The reaction mixture traversed through the catalyst bed, undergoing the desired reaction. Temperature regulation was achieved by situating the reactor inside a convection oven with precise temperature control. A back pressure regulator (100 psi) facilitated the regulation of pressure within the reactor, and subsequently, the product was collected at various time intervals for further analysis.

Product analysis

Samples underwent assessment *via* high-performance liquid chromatography (HPLC) to ascertain a range of reaction performance metrics. These included the % conversion of 5-HMF, % selectivity, % yield % productivity, and carbon balance, as detailed in eqn (1)–(5).

$$\%\ \text{Conversion of 5-HMF} = \left(1 - \frac{\dot{n}_{\text{5-HMF,f}}}{\dot{n}_{\text{5-HMF,ini}}}\right) \times 100 \quad (1)$$

$$\%\ \text{Yield} = \frac{\dot{n}_{\text{product}}}{\dot{n}_{\text{5-HMF,ini}}} \times 100 \quad (2)$$

$$\%\ \text{Selectivity} = \frac{\%\ \text{yield}}{\%\ \text{conversion}} \times 100 \quad (3)$$

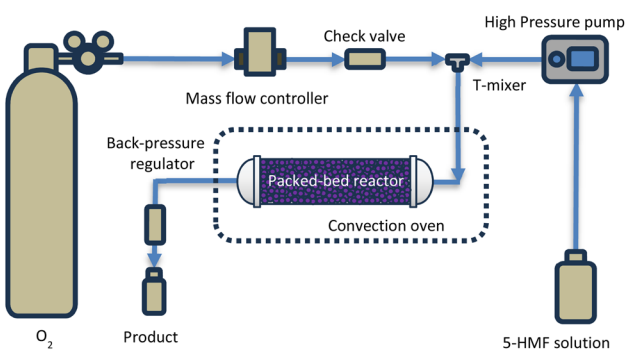

Fig. 1 The continuous process for DFF production.

$$\%\ \text{Productivity} = \frac{\%\ \text{yield} \times \dot{n}_{\text{5-HMF,ini}}}{m_{\text{cat}}} \quad (4)$$

$$\text{Carbon balance} = \frac{\sum \dot{n}_{\text{product}}}{\dot{n}_{\text{5-HMF,ini}} - \dot{n}_{\text{5-HMF,f}}} \times 100 \quad (5)$$

where $\dot{n}_{\text{5-HMF,f}}$ and $\dot{n}_{\text{5-HMF,ini}}$ represent the molar flow rate of 5-HMF in the feed and output stream, respectively. $\dot{n}_{\text{product}}$ is the molar flow rate of product such as DFF, HMFCA, FFCA, and FDCA.

The HPLC system employed for the analysis featured an ultraviolet detector (model 2550, Varian). The analysis was conducted using a reversed-phase C-18 column (Supelco, dimensions 250 mm × 4.6 mm) to quantify the levels of 5-HMF, DFF, HMFCA, FFCA, and FDCA. Column temperature was regulated at 50 °C using a column oven (model TCM-004076, Waters), while the mobile phase consisted of a mixture of ultrapure water (DI water), acetonitrile (ACN), and methanol (MeOH), with 0.025 M sulfuric acid (0.025 M H_2SO_4), in a ratio of 90 : 5 : 5 (DI : ACN : MeOH), flowing at a rate of 0.4 ml min^{-1}. Injection volume was set at 10 μL, and UV detection was performed at a wavelength of 270 nm.

Results

Characterization of catalyst

Fig. 2 displays X-ray diffraction patterns illustrating the distinct features of various catalysts. Analysis of the Pt/C spectrum reveals prominent peaks at 39.52, 45.59, and 67.18°, indicative of Pt crystallinity (ICDD 00-004-082), alongside a peak at 24.52° denoting crystalline carbon (ICDD 00-026-1077). Similarly, the Ru/C spectrum exhibits peaks at 38.52, 44.12, and 68.72° corresponding to crystalline Ru (ICDD 00-006-0663), with an additional peak at 25.23° representing crystalline carbon. The obtained crystallite size from Scherrer's equation[29] are 2.83 and 2.12 nm for Pt/C and Ru/C, respectively. In the Ru/Al_2O_3 spectrum, peaks at 37.23, 42.46, and 47.4° are attributed to γ-Al_2O_3 (ICDD 00-010-0425), while peaks at 36.49 and 43.22° signify metallic ruthenium. Furthermore, the textural properties of the catalysts were examined *via* N_2 adsorption–desorption isotherms and pulse H_2 chemisorption, detailed in Table 1. Notably, while Pt/C and Ru/C demonstrated comparable BET surface areas, Ru/Al_2O_3 exhibited a reduced surface area coupled with larger pore size.

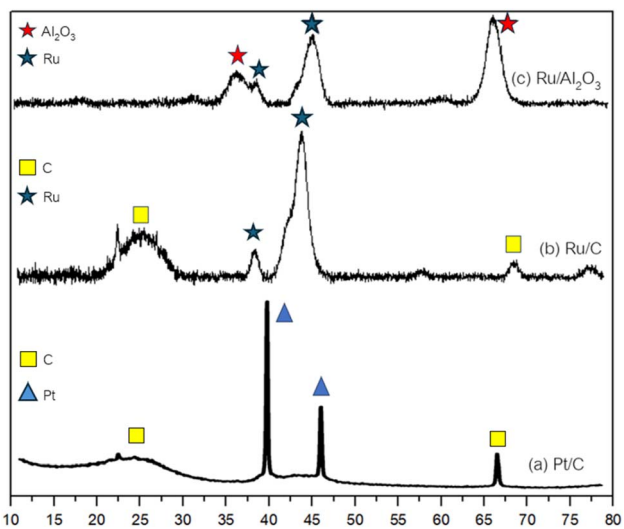

Fig. 2 The XRD pattern of catalyst (a) Pt/C, (b) Ru/C and (c) Ru/Al_2O_3.

The metal dispersion and total acid/base properties of the catalysts were investigated. Ru/Al_2O_3 exhibited comparable metal dispersion to Ru/C, whereas Pt/C displayed the lowest dispersion. This lower dispersion of Pt may have contributed to reduced catalytic activity, as a higher dispersion typically affords greater accessibility of reactant molecules to active sites.

Regarding acidity/basicity, Pt/C demonstrated the highest total acidity, suggesting its potential suitability for acid-catalyzed reactions. In contrast, Ru/Al_2O_3 exhibited the highest total basicity, likely attributed to the intrinsic basicity of the Al_2O_3 support, making it a promising candidate for base-catalyzed processes.

Fig. 3 presents SEM images of the Pt/C, Ru/C, and Ru/Al_2O_3 catalysts. Both Pt/C and Ru/C exhibited uniformly dispersed metal particles on a highly porous carbon support (Fig. 3a and b). In contrast, Ru/Al_2O_3 displayed a similar particle distribution but with a less porous Al_2O_3 support structure (Fig. 3c).

Fig. 4 displays the adsorption isotherms of the investigated catalysts. Pt/C and Ru/C exhibited type I isotherms, indicative of microporous structures, where monolayer adsorption predominates. Conversely, Ru/Al_2O_3 presented a type IV isotherm, characteristic of mesoporous materials, suggesting multilayer adsorption.

Effect of catalysts

In this study, three distinct catalysts (Pt/C, Ru/C, and Ru/Al_2O_3) were employed for the synthesis of DFF from 5-HMF. The experiments were conducted at a temperature of 120 °C, with a 5-HMF solution concentration of 5 g L^{-1} and a flow rate of 0.06 ml min^{-1}, utilizing acetonitrile as the solvent and oxygen gas at a flow rate of 10 ml min^{-1}. The catalyst amount used was 0.05 g. The outcomes are depicted in Fig. 5.

Table 1 The physical properties of catalysts

Catalyst	S_{BET} (m^2 g^{-1})	Pore volume (m^2 g^{-1})	Pore size (nm)	% Metal dispersion	Total acid site (μmol g^{-1})	Total basic site (μmol g^{-1})
Pt/C	1059.87	0.57	2.27	3.13	219.38	4.62
Ru/C	1059.37	0.57	2.27	7.57	170.68	8.57
Ru/Al_2O_3	212.92	0.58	10.61	6.89	45.58	28.17

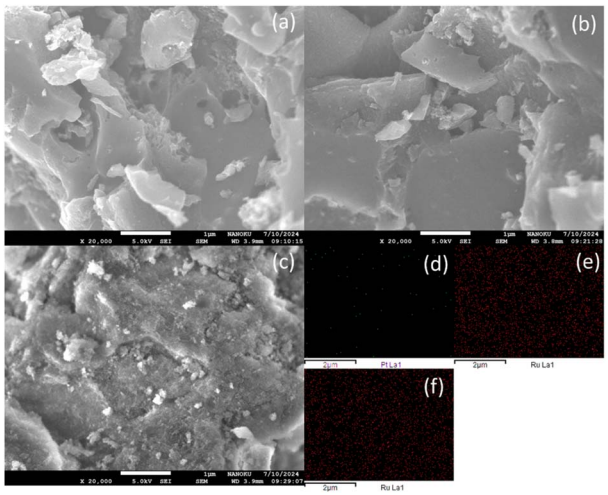

Fig. 3 SEM-DES of catalysts (a) Pt/C, (b) Ru/C, (c) Ru/Al_2O_3, (d) Pt particles on C, (e) Ru particles on C and (f) Ru particles on Al_2O_3.

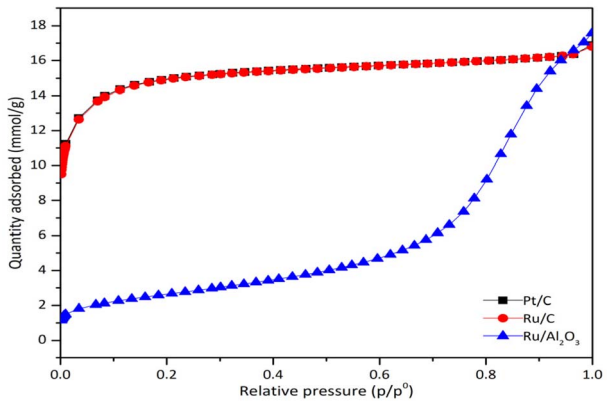

Fig. 4 Isotherm of catalysts.

Pt/C exhibited a low conversion rate of approximately 28% for 5-HMF and yielded only 4% DFF. This can be attributed to Pt/C's high activity for oxidation reactions under basic conditions, as previously reported by Rass *et al.* who also utilized Pt/C for FDCA synthesis.[30] It was observed that elevating the pH in the reaction environment enhanced FDCA yield. Hence, Pt/C's reactivity is diminished in free-base conditions.

Ru/Al_2O_3 and Ru/C catalysts yielded higher % conversion and % yield for DFF. Remarkably, Ru/Al_2O_3 outperformed Ru/C in both % conversion and % yield for DFF. This superiority can be attributed to Al_2O_3's basic properties, which promote oxidation reactions. Additionally, the high specific surface area of activated carbon (Ru/C) likely results in increased 5-HMF adsorption affinity compared to Al_2O_3-supported catalysts. Consequently, oligomeric byproducts may form, covering active catalyst sites and leading to undesirable reactions. This aligns with previous research by Artz *et al.* (2015), indicating strong 5-HMF adsorption on Ru/C surfaces at room temperature without undergoing oxidation reactions.[31]

Side reactions were evident in the system, indicated by the carbon balance. Notably, the carbon balance for Ru/Al_2O_3 was

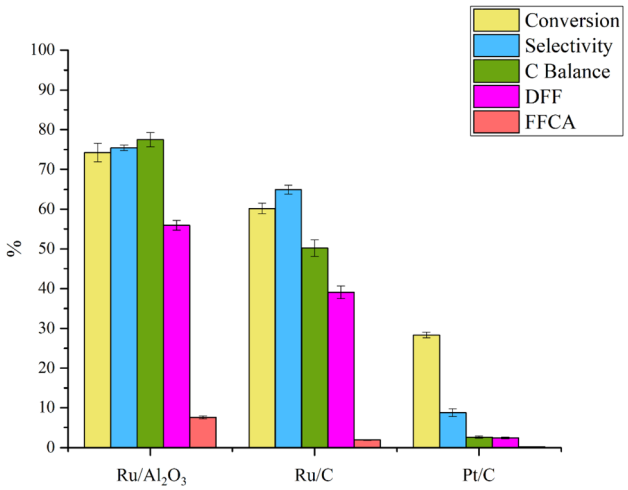

Fig. 5 Impact of catalyst types on reaction performance. Experimental conditions: temperature maintained at 120 °C, 5-HMF solution concentration of 5 g L^{-1}, flow rate of 0.06 ml min^{-1} for 5-HMF solution, acetonitrile utilized as the solvent, oxygen gas flow rate set at 10 ml min^{-1}, and catalyst quantity of 0.05 g.

approximately 78%, suggesting significant suppression of side reactions. Consequently, Ru/Al_2O_3 was selected for further exploration of operating condition effects in this study.

Effect of solvent

To explore the impact of solvents on the oxidation reaction of 5-HMF in a continuous flow reactor aimed at synthesizing DFF, a range of solvents including DI water, acetonitrile, DMSO, and toluene were individually employed. Results are summarized in Fig. 6. The experimental conditions included a reaction temperature of 120 °C, a flow rate of 5-HMF solution (5 g L^{-1})

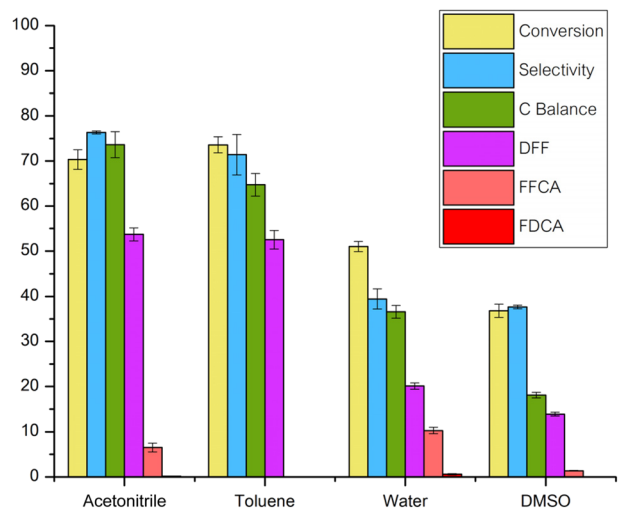

Fig. 6 Impact of solvent on reaction performance. Experimental conditions: temperature maintained at 120 °C, 5-HMF solution concentration of 5 g L^{-1}, flow rate of 0.06 ml min^{-1} for 5-HMF solution, oxygen gas flow rate set at 10 ml min^{-1}, and catalyst quantity of 0.05 g (Ru/Al_2O_3).

set at 0.06 ml min^{-1}, oxygen gas flow rate of 10 ml min^{-1}, and catalyst amount of 0.05 g, utilizing Ru/Al_2O_3 as the catalyst.

Observations revealed that employing DMSO as a solvent led to the lowest 5-HMF conversion and DFF yield. This may be attributed to DMSO's highly polar aprotic nature within the solvent category utilized in this study.[32,33] DMSO's weakly acidic properties could potentially catalyze the conversion of 5-HMF into higher molecular weight products, such as humins,[26] thereby diminishing its interaction with the catalyst, as suggested by Chen *et al.*'s investigation.[28]

Conversely, utilizing DI water as a solvent resulted in overly vigorous reactions due to its propensity for hydration reactions with the aldehyde functional groups of 5-HMF and DFF, leading to the formation of geminal diols.[26,29,34] Additionally, further oxidation reactions ensued, converting them into corresponding carboxylic acids like FFCA and FDCA. These compounds adhered to the catalyst surface, diminishing its activity and resulting in decreased % conversion and % yield.[27]

Both acetonitrile and toluene exhibited comparable reaction performances concerning 5-HMF conversion and DFF yield. However, acetonitrile as a solvent promoted the % yield of FFCA due to its superior oxidation potential compared to toluene.[33,35] Consequently, toluene was selected as the solvent for subsequent experiments in this study, as the formation of FFCA with acetonitrile would lead to compound deposition on the catalyst surface, reducing its reactivity over time. Moreover, the relatively lower cost of toluene enhances the economic feasibility of the process. Although toluene may raise environmental concerns, its recyclability in this process through vacuum-assisted evaporation followed by condensation offers a potential solution.

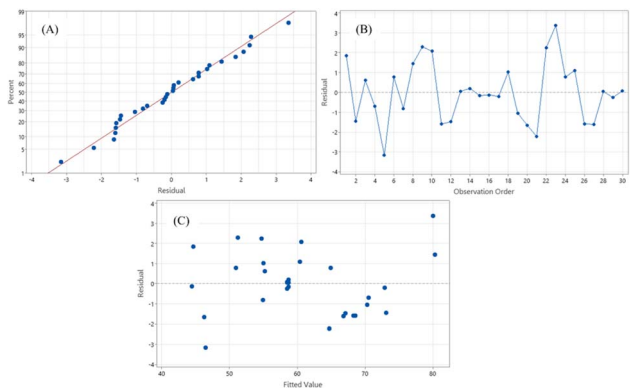

Fig. 7 Residual plots for DFF yield (A) normal probability of the residuals, (B) residuals *versus* the order of the data and (C) residuals *versus* the fitted values.

Optimization

The Box–Behnken Design (BBD) and response surface methodology (RSM) were utilized to explore the impacts of all variables on the response (dependent variable) and to optimize the operational conditions for synthesizing DFF from 5-HMF using Ru/Al_2O_3 as the catalyst in a continuous flow reactor. Examination of residual value distribution, as illustrated in Fig. 7A, indicates that the residuals of percentage yield are closely scattered around the straight line, suggesting a lack of abnormal patterns and allowing for the assumption of a normal distribution. To evaluate residual independence, a scatter plot was employed to observe the distribution characteristics of data points on the graph, as shown in Fig. 7B, revealing no discernible pattern in the residuals, indicating a lack of independence in the data. Assessment of variance stability *via* scatter plots of residuals at different factor levels, depicted in Fig. 7C, indicates a normal distribution of residuals in both positive and negative directions, suggesting stable variance within the data. Therefore, the experimental data is deemed accurate and suitable for analyzing the coefficient of determination (R^2).

In this investigation, three key variables influencing the oxidation reaction of 5-HMF were examined: temperature (X_1), the flow rate of oxygen gas (X_2), and the catalyst amount (X_3). Each variable was explored at three distinct levels: low (−1), medium (0), and high (+1). The yield of DFF (Y), a critical parameter indicating the quantity of DFF generated, was chosen as the response variable. The relationship between these factors and the response (Y; % yield of DFF) can be represented by a polynomial equation, as described in eqn (6).

$$Y = -4.5 + 0.113X_1 + 2.238X_2 - 137X_3 + 787{X_3}^2 - 0.01644X_1X_2 + 1.733X_1X_3 - 5.45X_2X_3 + 787{X_3}^2 \quad (6)$$

Table 2 Analysis of variance for main and interaction effects and the fitted polynomial regression model

Source	Degrees of freedom	Sum of squares	Mean squares	*p*-Value	Remark
X_1	1	1922.64	1922.64	0.000	Significant
X_2	1	63.08	63.08	0.000	Significant
X_3	1	567.61	567.61	0.000	Significant
X_1X_1	1	7.16	7.16	0.171	Not significant
X_2X_2	1	10.52	10.52	0.101	Not significant
X_3X_3	1	28.57	28.57	0.010	Significant
X_1X_2	1	86.45	86.45	0.000	Significant
X_1X_3	1	24.03	24.03	0.017	Significant
X_2X_3	1	59.31	59.31	0.001	Significant
R^2			97.63%		
R^2(adj)			96.38%		
R^2(pred)			93.24%		

The statistical significance of the model was evaluated using analysis of variance (ANOVA), detailed in Table 2. The fitted equation yielded a p-value below 0.05, indicating significance at a 95% confidence level. Table 2 summarizes the main and interaction factors alongside their corresponding p-values, highlighting factors with p-values less than 0.05 as statistically significant.

The coefficient of determination (R^2) quantifies the proportion of variability in the dependent variable explained by the independent variables in the regression equation. In this analysis, the R^2 value stands at 97.63%, indicating that the independent variables can account for 97.63% of the variability or changes in the dependent variable. This suggests the model's suitability for accurate predictions of DFF yield.

Utilizing the model, operating conditions for DFF synthesis from 5-HMF were optimized based on DFF yield. Under the identified optimal conditions (reaction temperature of 140 °C, oxygen flow rate of 10 ml min^{-1}, and catalyst quantity of 0.15 g), a DFF yield of 85.41% was achieved. To validate the prediction accuracy, the reaction was conducted at these optimal conditions, resulting in a DFF yield of 86.68%. This closely aligns with the predicted value, exhibiting a marginal deviation of 1.7%, which falls within an acceptable error margin (not exceeding 5%).

Effect of variables on the response

In Fig. 8a, we depict the combined influence of reaction temperature and oxygen flow rate on DFF yield in a continuous flow reactor containing 0.1 g of Ru/Al_2O_3 catalyst. Elevated reaction temperatures are shown to enhance DFF yield due to the increased rate of 5-HMF oxidation at higher temperatures. The effect of oxygen flow rate varies depending on the specific combination of reaction temperature and oxygen flow rate. At relatively low temperatures, an increase in DFF yield is noticeable with rising oxygen flow rates. The oxygen flow rate has a dual effect on 5-HMF conversion, positively impacting oxidation reactions by increasing oxygen content while decreasing contact time between reacting molecules and catalyst active sites. Consequently, the influence of oxygen flow rate on yield is relatively minor, particularly at high temperatures where reactions operate at high conversion levels. Examining the interaction between reaction temperature and catalyst quantity in DFF synthesis (Fig. 8b), simultaneous increases in both parameters result in higher DFF yield. This is attributed to the enhanced reaction rate with rising temperature and extended contact time with increased catalyst quantity. For instance, tripling the catalyst amount effectively triples contact time, facilitating a more favorable interaction between 5-HMF and catalyst, thereby improving DFF yield.

Fig. 8c illustrates the combined impact of oxygen flow rate and catalyst quantity. An increase in DFF yield is observed with higher oxygen flow rates when catalyst amount is low, but this effect diminishes with larger catalyst quantities, particularly in high conversion regions. The positive effect of increased oxygen flow is overshadowed by high 5-HMF conversion. For instance, elevating the oxygen flow rate from 10 to 30 ml min^{-1} resulted in a decrease of 0.54 seconds (63%) in contact time, yet the DFF

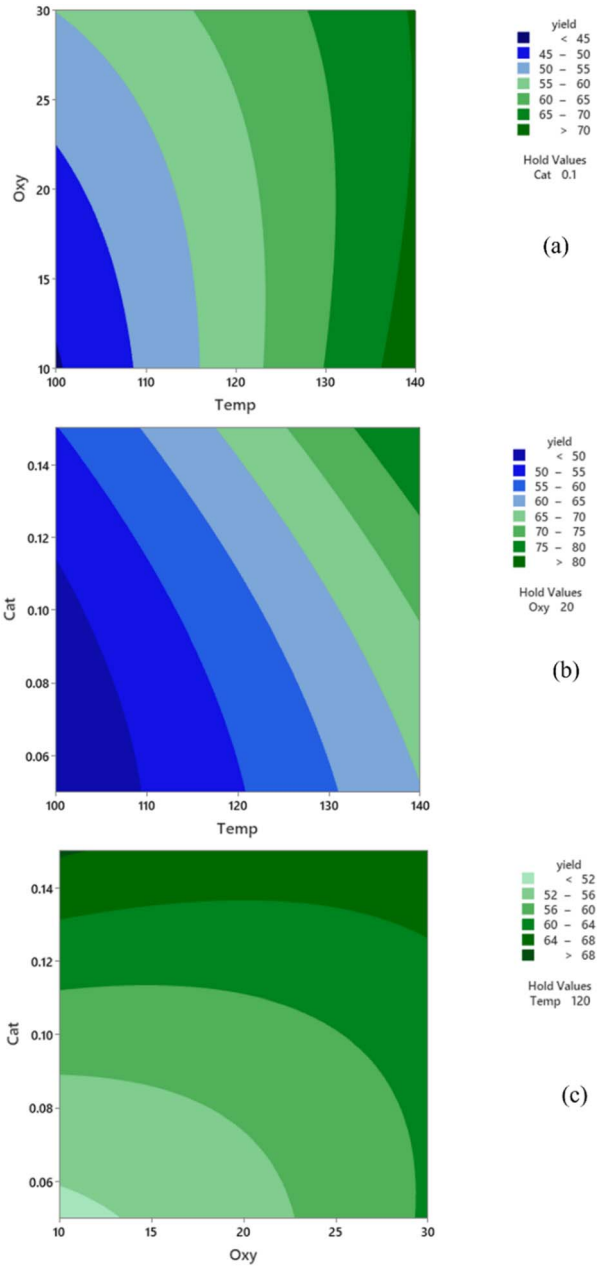

Fig. 8 Response surface and contour plots illustrating the yield of DFF utilizing the Box–Behnken design, achieved by plotting (a) oxygen flow rate *versus* reaction temperature, (b) catalyst amount *versus* reaction temperature, and (c) catalyst amount *versus* oxygen flow rate.

yield remained relatively constant. Conversely, the impact is significant when both oxygen flow rate and catalyst quantity are low, operating in low conversion regions. However, the cost of catalyst, a significant contributor to production costs, necessitates careful consideration when selecting operating conditions. For instance, achieving a 64% yield required a catalyst amount of 0.05 g with an oxygen flow rate of 30 ml min^{-1}.

Purification of DFF

The crude DFF product obtained from 5-HMF oxidation was purified by rotary evaporation at 60 °C under a vacuum of −14.5

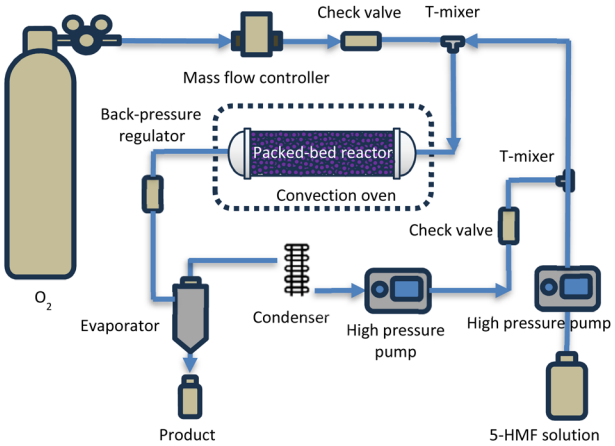

Fig. 9 Schematic diagram illustrating the conceptual production process of DFF.

psi. Subsequent HPLC analysis against a DFF standard indicated a purity of 87%. To enhance process sustainability and economic viability, solvent recycling was implemented to significantly reduce toluene consumption. Despite toluene's environmental concerns, its volatility enabled effective recovery and reuse. A schematic representation of the integrated DFF production process incorporating solvent recycling is presented in Fig. 9. This continuous process produces high-purity DFF suitable for practical applications. The crude DFF stream from the packed-bed reactor is fed to the evaporator. The purified product is collected, while the condensed toluene vapor was recycled by reintroduction into the 5-HMF feed solution using a high-pressure pump.

Stability of catalyst

The catalyst's stability was evaluated by conducting reactions under optimal conditions for DFF synthesis from 5-HMF:

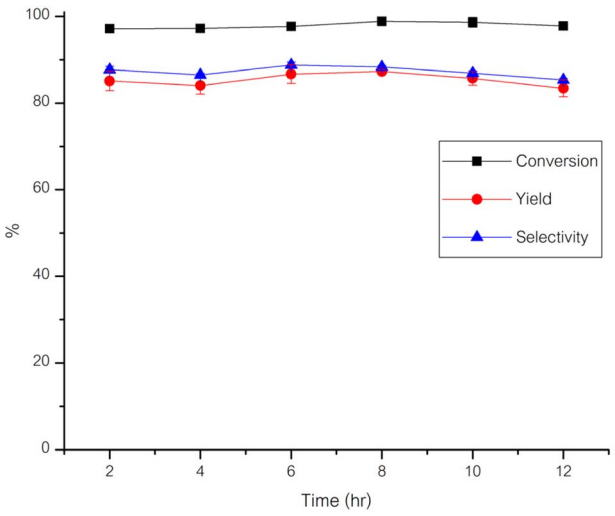

Fig. 10 Reaction performance of DFF synthesis over Ru/Al_2O_3 catalyst over an extended period.

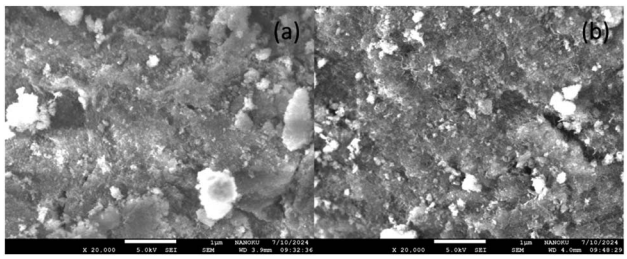

Fig. 11 SEM of (a) fresh and (b) spent catalysts.

a temperature of 120 °C, an oxygen flow rate of 10 ml min^{-1}, and a catalyst amount of 0.15 g. Product was collected every 2 h throughout the experiment, with results depicted in Fig. 10. Following a 12 h duration, the percentage yield of 5-HMF decreased from 86.86% to 83.44%, marking a 3.7% reduction. This suggests that the Ru/Al_2O_3 catalyst remained relatively stable under optimal conditions for DFF production in the continuous flow reactor.

A comparison of the spent (optimal conditions) and fresh catalysts revealed a minimal decrease in surface area from 212.92 to 199.59 m^2 g^{-1}. Furthermore, the SEM images in Fig. 11 demonstrate that the morphology of the spent catalyst remained largely intact, indicating the catalyst's durability. The diminishing DFF yield over time may be attributed to polymerization reactions, leading to humins formation. Consequently, these species partially cover the catalyst's active sites, impeding reactions as time-on-stream increases. Antonyraj *et al.*[27] employed Ru/Al_2O_3 as a catalyst for DFF synthesis from 5-HMF. Upon analyzing the spent catalyst using IR analysis techniques, organic substances adsorbed on the catalyst surface were observed. This inhibition of oxidation reactions resulted in decreased 5-HMF conversion and DFF yield. However, treatment with NaOH followed by subsequent reaction revealed the catalyst's regained efficiency in effectively promoting the reaction.

Comparison of process performance

The performance of our system in terms of 5-HMF conversion, DFF yield, reaction time, and productivity under optimal conditions was compared with literature data, as summarized in Table 3. Previous research primarily utilized batch reactors, known to require longer reaction times compared to packed-bed reactors to achieve similar conversions. Tong *et al.*[38] synthesized DFF from 5-HMF using the CuI + HBT catalytic system, yielding a conversion and selectivity of 93.2% and 99%, respectively. However, despite the reaction time extending up to 10 h, productivity remained relatively low. In continuous flow reactor systems, reaction times (residence times) can be significantly shorter than those in batch systems due to minimal back-mixing, facilitating rapid reactions and potentially superior productivity, as demonstrated in Table 3.

Chen *et al.* conducted DFF synthesis from 5-HMF using CuZnAl as the catalyst in a continuous flow reactor.[28] Although productivity improved considerably compared to batch systems, reaction temperature needed to be raised to 260 °C. Water was

Table 3 Comparison of DFF synthesis using different systems

Catalyst	Reaction conditions (temperature/reaction time/solvent)	Conversion (%)	Selectivity (%)	Productivity ($mol_{DFF}\ g_{cat.}^{-1}\ h^{-1}$)	Reactor
α-MnO_2	140 °C/4 h/isopropanol	93.2	84.3	3.9×10^{-3}	Batch[36]
α-MnO_2	140 °C/4 h/H_2O	60.9	78.2	2.4×10^{-3}	Batch[36]
α-MnO_2	140 °C/4 h/acetonitrile	81.2	76.8	3.1×10^{-3}	Batch[36]
Mn_6FeO_x	110 °C/5 h/DMF	97	98	2.3×10^{-3}	Batch[37]
$MgOMnO_2CeO_2$	110 °C/10 h/H_2O	98.8	95.2	2.1×10^{-4}	Batch[34]
CuI + HBT	130 °C/10 h/DMSO	93.2	99	9.2×10^{-5}	Batch[38]
1.8 wt% Ru/Al_2O_3	120 °C/4 h/toluene	100	97	1.3×10^{-3}	Batch[27]
CuZnAl	260 °C/0.75 h/H_2O	67.6	48.1	0.016	Flow[28]
5 wt% Ru/Al_2O_3	140 °C/1.04 s/toluene	99	85.05	2.0016	Flow

employed as a solvent in their research to effectively facilitate oxidation reactions. However, overoxidation and side reactions led to relatively low selectivity (48.1%) and productivity (0.016 $mol_{DFF}\ g_{cat.}^{-1}\ h^{-1}$). Our study utilized Ru/Al_2O_3, which remains active even at lower temperatures. Operating at 140 °C significantly reduces energy consumption compared to 260 °C. High conversion and selectivity were achieved within a residence time of 1.04 s, resulting in much higher productivity (2.0016 $mol_{DFF}\ g_{cat.}^{-1}\ h^{-1}$) compared to literature data.

Compared to other studies, our findings have the potential to enhance production capacity and be applied to large-scale industrial DFF production from 5-HMF. This is due to shorter reaction times, relatively lower reaction temperatures, high DFF yield and selectivity, as well as the high stability and productivity of the catalyst used in our study compared to literature sources.

Conclusion

In this study, the synthesis of DFF from 5-HMF utilizing catalytic reaction acceleration in a continuous flow reactor was explored across various parameters, including catalyst type (Pt/C, Ru/C, Ru/Al_2O_3), reaction temperature (100–140 °C), oxygen gas flow rate (10–30 ml min^{-1}), and catalyst quantity (0.05–0.15 g). Optimization of operating conditions was conducted using the Box–Behnken Design (BBD) method in conjunction with Response Surface Methodology (RSM), elucidating the impact of these conditions and identifying the best parameters through predictive modeling. The yield of DFF was notably influenced by reaction temperature, oxygen gas flow rate, and catalyst quantity, both individually and through their interaction effects. Optimal conditions for DFF synthesis in the continuous flow reactor were determined to be a temperature of 140 °C, an oxygen gas flow rate of 10 ml min^{-1}, and a catalyst quantity of 0.15 g. The exceptional productivity achieved in the continuous flow reactor employing Ru/Al_2O_3 catalyst under these optimal conditions was confirmed and benchmarked against existing literature data.

Data availability

The data supporting this article have been included as part of the ESI.†

Conflicts of interest

There are no conflicts to declare.

Acknowledgements

The authors acknowledge the financial support from the 2-Institution Co-Research Scholarship provided by Kasetsart University and National Chung Hsing University, grant No. 32022.

Notes and references

1 A. Corma, S. Iborra and A. Velty, Chemical Routes for the Transformation of Biomass into Chemicals, *Chem. Rev.*, 2007, **107**, 2411–2502.
2 D. M. Alonso, J. Q. Bond and J. A. Dumesic, Catalytic conversion of biomass to biofuels, *Green Chem.*, 2010, **12**, 1493–1513.
3 P. Gallezot, Conversion of biomass to selected chemical products, *Chem. Soc. Rev.*, 2012, **41**, 1538–1558.
4 C. Bai, Q. Hou, X. Bai, Y. Nie, H. Qian, M. Zhen and M. Ju, Conversion of Glucose to 5-Hydroxymethylfurfural at High Substrate Loading: Effect of Catalyst and Solvent on the Stability of 5-Hydroxymethylfurfural, *Energy Fuels*, 2020, **34**, 16240–16249.
5 Y. Meng, S. Yang and H. Li, Electro- and Photocatalytic Oxidative Upgrading of Bio-based 5-Hydroxymethylfurfural, *ChemSusChem*, 2022, **15**(13), e202102581.
6 H. Li, Q. Zhang, P. S. Bhadury and S. Yang, Furan-type Compounds from Carbohydrates *via* Heterogeneous Catalysis, *Curr. Org. Chem.*, 2014, **18**, 547–597.
7 H. Wang, C. Zhu, D. Li, Q. Liu, J. Tan, C. Wang, C. Cai and L. Ma, Recent advances in catalytic conversion of biomass to 5-hydroxymethylfurfural and 2,5-dimethylfuran, *Renewable Sustainable Energy Rev.*, 2019, **103**, 227–247.
8 S. Xu, P. Zhou, Z. Zhang, C. Yang, B. Zhang, K. Deng, S. Bottle and H. Zhu, Selective Oxidation of 5-Hydroxymethylfurfural to 2,5-Furandicarboxylic Acid Using O_2 and a Photocatalyst of Co-thioporphyrazine Bonded to g-C_3N_4, *J. Am. Chem. Soc.*, 2017, **139**, 14775–14782.

9 A. Gandini and N. M. Belgacem, Recent advances in the elaboration of polymeric materials derived from biomass components, *Polym. Int.*, 1998, **47**, 267–276.

10 M. D. Poeta, W. A. Schell, C. C. Dykstra, S. K. Jones, R. R. Tidwell, A. Kumar, D. W. Boykin and J. R. Perfect, In Vitro Antifungal Activities of a Series of Dication-Substituted Carbazoles, Furans, and Benzimidazoles, *Antimicrob. Agents Chemother.*, 1998, **42**, 2503–2510.

11 K. T. Hopkins, W. D. Wilson, B. C. Bender, D. R. McCurdy, J. E. Hall, R. R. Tidwell, A. Kumar, M. Bajic and D. W. Boykin, Extended Aromatic Furan Amidino Derivatives as Anti-Pneumocystis carinii Agents, *J. Med. Chem.*, 1998, **41**, 3872–3878.

12 A. S. Amarasekara, D. Green and L. D. Williams, Renewable resources based polymers: Synthesis and characterization of 2,5-diformylfuran–urea resin, *Eur. Polym. J.*, 2009, **45**, 595–598.

13 J. Ma, Z. Du, J. Xu, Q. Chu and Y. Pang, Efficient Aerobic Oxidation of 5-Hydroxymethylfurfural to 2,5-Diformylfuran, and Synthesis of a Fluorescent Material, Chemistry-Sustainability-Energy-Materials, *ChemSusChem*, 2011, **4**, 51–54.

14 O. C. Navarro, A. C. Canós and S. I. Chornet, Chemicals from Biomass: Aerobic Oxidation of 5-Hydroxymethyl-2-Furaldehyde into Diformylfurane Catalyzed by Immobilized Vanadyl-Pyridine Complexes on Polymeric and Organofunctionalized Mesoporous Supports, *Top. Catal.*, 2009, **52**, 304–314.

15 C. Carlini, P. Patrono, A. M. R. Galletti, G. Sbrana and V. Zima, Selective oxidation of 5-hydroxymethyl-2-furaldehyde to furan-2,5-dicarboxaldehyde by catalytic systems based on vanadyl phosphate, *Appl. Catal., A*, 2005, **289**, 197–204.

16 C. Moreau, R. Durand, C. Pourcheron and D. Tichit, Selective oxidation of 5-hydroxymethylfurfural to 2,5-furan-dicarboxaldehyde in the presence of titania supported vanadia catalysts, *Stud. Surf. Sci. Catal.*, 1997, **108**, 399–406.

17 J. Nie and H. Liu, Aerobic oxidation of 5-hydroxymethylfurfural to 2,5-diformylfuran on supported vanadium oxide catalysts: Structural effect and reaction mechanism, *Pure Appl. Chem.*, 2011, **84**, 765–777.

18 A. Takagaki, M. Takahashi, S. Nishimura and K. Ebitani, One-Pot Synthesis of 2,5-Diformylfuran from Carbohydrate Derivatives by Sulfonated Resin and Hydrotalcite-Supported Ruthenium Catalysts, *ACS Catal.*, 2011, **1**, 1562–1565.

19 Z.-Z. Yang, J. Deng, T. Pan, Q.-X. Guoa and Y. Fu, A one-pot approach for conversion of fructose to 2,5-diformylfuran by combination of Fe_3O_4-SBA-SO_3H and K-OMS-2, *Green Chem.*, 2012, **14**, 2986–2989.

20 B.-C. Li, J. Lee, E. Kwon, B. X. Thanh, J.-Y. Lin, S. You, C.-H. Lin and K.-Y. A. Lin, 2-dimensional nanoleaf-like porous copper nitrate hydroxide as an effective heterogeneous catalyst for selective oxidation of hydroxymethylfurfural to diformylfuran, *J. Taiwan Inst. Chem. Eng.*, 2021, **126**, 189–196.

21 S. Li, K. Su, Z. Li and B. Cheng, Selective oxidation of 5-hydroxymethylfurfural with H_2O_2 catalyzed by a molybdenum complex, *Green Chem.*, 2016, **18**, 2122–2128.

22 X.-h. Zhou, K.-h. Song, Z.-h. Li, W.-m. Kang, H.-r. Ren, K.-m. Su, M.-l. Zhang and B.-w. Cheng, The excellent catalyst support of Al_2O_3 fibers with needle-like mullite structure and HMF oxidation into FDCA over CuO/Al_2O_3 fibers, *Ceram. Int.*, 2018, **45**, 2330–2337.

23 A. S. Amarasekara, D. Green and E. McMillan, Efficient oxidation of 5-hydroxymethylfurfural to 2,5-diformylfuran using Mn(III)–salen catalysts, *Catal. Commun.*, 2008, **9**, 286–288.

24 W. Partenheimer and V. V. Grushin, Synthesis of 2,5-Diformylfuran and Furan-2,5-Dicarboxylic Acid by Catalytic Air-Oxidation of 5-Hydroxymethylfurfural. Unexpectedly Selective Aerobic Oxidation of Benzyl Alcohol to Benzaldehyde with Metal/Bromide Catalysts, *Adv. Synth. Catal.*, 2001, **343**, 102–111.

25 C. Moreau, M. N. Belgacem and A. Gandini, Recent Catalytic Advances in the Chemistry of Substituted Furans from Carbohydrates and in the Ensuing Polymers, *Top. Catal.*, 2004, **27**, 11–30.

26 J. Nie, J. Xie and H. Liu, Efficient aerobic oxidation of 5-hydroxymethylfurfural to 2,5-diformylfuran on supported Ru catalysts, *J. Catal.*, 2013, **301**, 83–91.

27 C. A. Antonyraj, J. Jeong, B. Kim, S. Shin, S. Kim, K.-Y. Lee and J. K. Cho, Selective oxidation of HMF to DFF using Ru/γ-alumina catalyst in moderate boiling solvents toward industrial production, *J. Ind. Eng. Chem.*, 2013, **19**, 1056–1059.

28 B. Chen, X. Li, P. Rui, Y. Ye, T. Ye, R. Zhou, D. Li, J. H. Carter and G. J. Hutchings, The reaction pathways of 5-hydroxymethylfurfural conversion in a continuous flow reactor using copper catalysts, *Catal. Sci. Technol.*, 2022, **12**, 3016–3027.

29 H. Huy, *et al.*, Preparation and characterization of high-dispersed pt/c nano-electrocatalysts for fuel cell applications, *J. Sci. Technol.*, 2016, **54**, 272–282.

30 H. A. Rass, N. Essayem and M. Besson, Selective aqueous phase oxidation of 5-hydroxymethylfurfural to 2,5-furandicarboxylic acid over Pt/C catalysts: influence of the base and effect of bismuth promotion, *Green Chem.*, 2013, 152240–152251.

31 J. Artz, S. Mallmann and R. Palkovits, Selective aerobic oxidation of HMF to 2,5-diformylfuran on covalent triazine frameworks-supported Ru catalysts, *ChemSusChem*, 2015, **8**, 672–679.

32 F. G. Bordwell, Equilibrium acidities in dimethyl sulfoxide solution, *Acc. Chem. Res.*, 1988, **21**, 456–463.

33 N. K. Gupta, S. Nishimura, A. Takagakib and K. Ebitani, Hydrotalcite-supported gold-nanoparticle-catalyzed highly efficient base-free aqueous oxidation of 5-hydroxymethylfurfural into 2,5-furandicarboxylic acid under atmospheric oxygen pressure, *Green Chem.*, 2011, **13**, 824–827.

34 F. Nocito, M. Ventura, M. Aresta and A. Dibenedetto, Selective Oxidation of 5-(Hydroxymethyl)furfural to DFF

Using Water as Solvent and Oxygen as Oxidant with Earth-Crust-Abundant Mixed Oxides, *ACS Omega*, 2018, **3**, 18724–18729.

35 Y. Y. Gorbanev, S. K. Klitgaard, J. M. Woodley, C. H. Christensen and A. Riisager, Gold-Catalyzed Aerobic Oxidation of 5-Hydroxymethylfurfural in Water at Ambient Temperature, *ChemSusChem*, 2009, **2**, 672–675.

36 L. Yu, H. Chen, Z. Wen, M. Jin, Z. Ma, X. Ma, Y. Sang, M. Chen and Y. Li, Highly selective oxidation of 5-hydroxymethylfurfural to 2,5-diformylfuran over an α-MnO_2 catalyst, *Catal. Today*, 2021, **367**, 9–15.

37 T. Kitamura, Synthetic Methods for the Generation and Preparative Application of Benzyne, *Aust. J. Chem.*, 2010, **63**, 987–1001.

38 X. Tong, Y. Sun, X. Baia and Y. Li, Highly Efficient Aerobic Oxidation of Biomass-derived 5-Hydroxymethyl Furfural to Produce 2,5-Diformylfuran in the Presence of Copper Salts, *RSC Adv.*, 2014, **83**, 44307–44311.